

Ultrasound-assisted synthesis of α -aminophosphonates using nano ZnO catalyst: evaluation of their anti-diabetic activity

Meson Haji Basha ^{1,2}, Chennamsetty Subramanyam ¹,

C. Gladis Raja Malar ³, Katare Kiran Kumar ⁴, Mohan Seelam ¹,

Vedula Naga Lakshmi ⁵ and Kammela Prasada Rao ^{1*}

¹Department of Chemistry (recognized as research centre by A.N. University), Bapatla Engineering College (Autonomous), Bapatla, Andhra Pradesh, India -522101

²Department of Chemistry, Acharya Nagarjuna University, Guntur, Andhra Pradesh, India -522510

³Department of Chemistry, Vel Tech Multi Tech Dr.Rangarajan Dr.Sakunthala Engineering College, Avadi, Chennai, Tamil Nadu, India-600062

⁴Department of Chemistry, K. B. N. College (A), kotha pet, Vijayawada -520001 Andhra Pradesh, India -534007

⁵Department of Chemistry, Ch.S.D.St.Theresa's College for Women (A), Eluru, Andhra Pradesh, India-534003

(Received December 17, 2024; Revised December 28, 2024; Accepted December 29, 2024)

Abstract: A more efficient and environmentally friendly way of synthesizing α -aminophosphonates is achieved by employing nano-ZnO to catalyze the Kabachnik-Fields reaction under ultrasonication within a solvent-free environment. Before synthesis, molecular docking and in silico ADME analysis were used to assess each molecule's drug-like characteristics and ability to inhibit α -amylase and α -glucosidase. The newly synthesized compounds' *in vitro* inhibitory effects on α -amylase and α -glucosidase were also evaluated, and their structure was confirmed using spectroscopic investigation. The target enzyme was effectively inhibited by most of the substances. In comparison to the reference drug, acarbose (IC₅₀, 106.5±0.6 µg/mL), compounds **4d** (IC₅₀, 102.2±0.3 µg/mL), **4h** (IC₅₀, 102.9±0.4 µg/mL), which contained a 2H-1,3-benzodioxol-5-yl moiety, and **4i** (IC₅₀, 103.9±0.5 µg/mL) showed the strongest inhibitory activity. The enzyme inhibition of the remaining compounds ranged from moderate to good.

Keywords: Kabachnik-Fields reaction; α -aminophosphonates; ADMET; molecular docking; α -amylase; α -glucosidase. © 2024 ACG Publications. All rights reserved.

1. Introductions

Diabetes mellitus (DM) has emerged as a serious global health concern, with an estimated 537 million individuals living with the condition by 2021. This figure is expected to rise to 783 million by 2045, placing a substantial economic and social strain on global healthcare systems.¹

Diabetes is defined by chronic hyperglycemia caused by abnormalities in insulin production, insulin action, or both, and it is a major cause of morbidity and mortality because of its related consequences, which include cardiovascular disease, neuropathy, nephropathy, and retinopathy. Controlling postprandial blood glucose (PPG) levels is crucial in diabetes management since increased PPG raises the risk of microvascular and macrovascular problems.²

* Corresponding author:-E-Mail: prasad17467@gmail.com

The enzymes α -amylase and α -glucosidase are essential in carbohydrate metabolism. α -Amylase breaks down starch into smaller oligosaccharides, while α -glucosidase converts these oligosaccharides into absorbable monosaccharides like glucose. The inhibition of these enzymes slows carbohydrate digestion, resulting in a controlled and progressive release of glucose into the bloodstream, minimizing postprandial hyperglycemia. Existing α -amylase and α -glucosidase inhibitors, such as acarbose, voglibose, and miglitol, are therapeutically efficacious, but sometimes associated with gastrointestinal side effects, including flatulence and diarrhea, limiting their widespread usage.³ Thus, the discovery of new inhibitors with increased efficacy and fewer adverse effects remains an important topic of research.

In addition to experimental procedures, *in silico* investigations have proven essential in current drug discovery. These computational tools allow for the detection of molecular interactions, prediction of binding affinities, and investigation of structure-activity connections. Molecular docking and simulation studies give information on the binding processes of prospective inhibitors to target enzymes, enabling the rational design and optimization of therapeutic candidates. Furthermore, *in silico* approaches enhance experimental research by saving time and resources, directing synthetic efforts, and identifying good candidates for biological evaluation.⁴

On the other hand, chemical processes known as multicomponent reactions (MCRs)⁵⁻⁸ occur when several substrates react at the same time to produce a single product that contains components of each reactant. MCRs have several benefits over stepwise reactions in the field of green chemistry, including as high atom economy, step efficiency, exploratory diversity, and the avoidance of intermediate purification. As a result, they are thought to be crucial instruments in diversity-oriented synthesis and fit in nicely with ecologically friendly synthesis procedures.^{9,10}

Notable biological properties of bis(α -aminophosphonates) include antioxidant,¹¹ anti-tubercular,¹² anti-diabetic,¹³ and anti-proliferative activity against human tumor cells from colon carcinoma.¹⁴ They are useful ligands for extracting metals, monomers for synthesizing macrocyclic compounds, and building blocks for polymers that contain amines and phosphonates.¹⁵ Their synthesis from diamines,^{16,17} dialdehydes,^{18,19} Brønsted and Lewis acids,²⁰ bases,^{21,22} Schiff bases,²³⁻²⁵ and organocatalysts²⁶ has been investigated using a variety of synthetic methods. Long reaction periods, large catalyst amounts, and poor diastereoisomer ratios are still problems in spite of these techniques. Therefore, the development of novel bis(α -aminophosphonates) requires innovative and effective synthesis routes.

Among the various synthetic techniques suggested for the production of α -Aps, the Kabachnik-Fields (K-F) reaction—the nucleophilic addition of phosphites to imines was demonstrated to be a practical method.²⁷ Many techniques have been devised to synthesize α -Aps utilizing this reaction,²⁸⁻³⁴ but some of the current methods have problems including needing solvents, taking a long time to react, and requiring expensive catalysts. Therefore, a more effective, simple, and high-yielding synthesis protocol for these molecules is still needed. Over the past few decades, ultra-sonication has become a useful technique in organic synthesis. For processes that normally demand for heating, it provides an alternate energy source that improves reaction speeds, yields, and selectivity. Ultrasound promotes organic transformations at ambient temperatures, avoiding the requirement for harsh conditions like as high temperature and pressure, which is very useful for synthesizing α -Aps.^{35,36}

Nanoparticles such as zinc oxide (nano ZnO) have sparked widespread interest due to its beneficial properties such as low toxicity, cost-effectiveness, compatibility with air and water, and recycling.³⁷⁻⁴² We wanted to study the possibility of a one-pot three-component reaction for α -Aps formation, given its advantages and ongoing research into novel α -AP synthesis techniques.⁴³⁻⁴⁸

The main goal of this study is to create a new ultrasound-assisted synthesis method for α -aminophosphonates using a nano ZnO catalyst and assess its inhibitory effect against α -amylase and α -glucosidase. Using *in vitro* tests, the study also aims to investigate the synthetic substances' probable anti-diabetic potential. The binding associations of these drugs with the α -amylase and α -glucosidase active sites will also be examined using molecular docking experiments, which will provide mechanistic insights into their inhibitory effects. The goal of this research is to help discover safer and more effective therapeutic molecules for the treatment of diabetes by combining synthetic chemistry, biological evaluation, and *in silico* analysis.

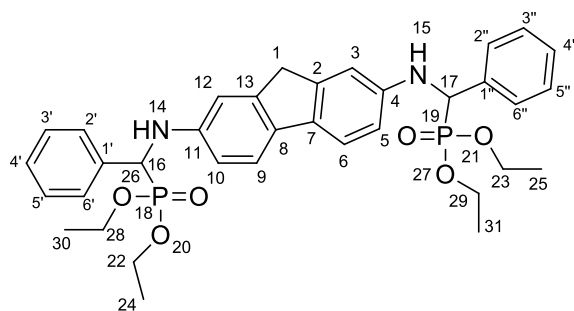
2. Experimental

2.1. Procedures

2.1.1. Ultrasound Assisted Synthesis of α -aminophosphonates (**4a-j**)

In a flat-bottomed flask, benzaldehyde (**1a**) (2.04 mL, 0.020 mol), 9H-fluorene-2,7-diamine (**2**) (1.96g, 0.010 mol), and diethyl phosphite (**3**) (1.3 mL, 0.020 mol) were mixed. Nano ZnO (5 mol%) was added to the mixture, and ultrasonication was performed for 5 minutes at room temperature under solvent-free conditions. The reaction's development was evaluated using TLC (ethyl acetate: n-hexane, 6:4). The reaction mixture was cooled to room temperature after TLC analysis confirmed that it was complete. Dichloromethane (DCM) (15 mL) was then added to the reaction mixture and stirred for 10 minutes. The catalyst, nano ZnO, was filtered, washed with DCM (2×10 mL), and dried under vacuum at 100°C for later use. The crude product was produced by washing the mixed organic layer with 15 mL of water, drying it over anhydrous Na₂SO₄, and concentrating it under vacuum at 50°C. Tetraethyl (((9H-fluorene-2,7-diyl)bis(azanediyl))bis(phenylmethylene))bis(phosphonate) (**4a**) was then synthesized using ethyl acetate:n-hexane (3:2) as an eluetae. The compounds (**4b-j**) were produced using the same method.

2.2. Characterization of title compounds (**4a-j**)



Compound **4a**

Tetraethyl (((9H-fluorene-2,7-diyl)bis(azanediyl))bis(phenylmethylene))bis(phosphonate) (**4a**): M.F.: C₃₅H₄₂N₂O₆P₂; Yield: 95%; Solid. M.P.178-180 °C. ¹H NMR spectrum (400 MHz, DMSO-d₆): δ 7.58 (d, *J*= 7.6 Hz, 2H, Ar-H), 7.17 (t, *J*= 7.2 Hz, 4H, Ar-H), 7.09 (t, *J*= 6.8 Hz, 2H, Ar-H), 7.02 (d, *J*= 7.6 Hz, 4H, Ar-H), 6.81 (s, 2H, Ar-H), 6.63 (d, *J*= 7.6 Hz, 2H, Ar-H), 5.42 (s, 2H, NH), 4.39 (m, 4H, -O-CH₂CH₃), 4.08 (m, 2H, -O-CH₂CH₃), 3.95 (d, *J*= 16 Hz, 2H, P-CH), 3.91 (m, 2H, -O-CH₂CH₃), 3.73 (s, 2H, -CH₂), 1.27 (t, *J*= 6.8 Hz, 6H, -O-CH₂CH₃), 1.13 (t, *J*= 6.8 Hz, 6H, -O-CH₂CH₃); ¹³C NMR spectrum (100 MHz, DMSO-d₆): δ 146.4 (C-4, C-11), 141.4 (C-2, C-13), 134.6 (C-1', C-1''), 128.8 (C-7, C-8), 128.1 (C-6, C-9), 127.5 (C-3', C-3'', C-5', C-5''), 126.2 (C-2', C-2'', C-6', C-6''), 125.4 (C-4', C-4''); 111.6 (C-3, C-12), 110.8 (C-5, C-10), 64.07 (d, *J*= 5.2 Hz, C-22 & C-28), 62.85 (d, *J*= 5.0 Hz, C-23 & C-29), 56.71 (d, *J*= 104 Hz, C-16 & C-17), 37.3 (C-1), 14.85 (d, *J*= 5.1 Hz, C-24 & C-30), 13.88 (d, *J*= 10.2 Hz, C-25 & C-31); ³¹P NMR (161.9 MHz, DMSO-d₆): δ 15.2 ppm. IR (KBr) (ν_{max} cm⁻¹): 3241 (NH), 1231 (P=O), 1007 (P-O-C_{alip}); LCMS (m/z, %): 649 (M+H⁺,100). Anal. Calcd: C, 64.81; H, 6.53; N, 4.32%. Found: C, 64.91; H, 6.42; N, 4.43%. The spectral data of compounds **4b-j** is available in supporting information of the article.

2.3. In-silico Analysis

The physicochemical, lipophilicity, water solubility, pharmacokinetic/ADME, drug-likeness, and medicinal chemistry of each of the proposed compounds were all inferred using the Swiss ADME tool from the Swiss Institute of Bioinformatics (<http://www.sib.swiss>).

2.4. In-silico molecular docking studies

The binding mechanism of **4a-j** with the targeted enzymes, pancreatic α -amylase (PDB ID: 3IJ8) and α -glucosidase (PDB ID: 1OBB), was investigated using in silico molecular docking. The RCSB, Protein Data Bank (PDB ID: 3IJ8, 1OBB) was used to obtain the crystal structures of both enzymes. Heteroatoms, co-factors, and water molecules were removed from the structure to increase efficiency. Missing atoms, hydrogen bonds, and charges were introduced. The 1-Click docking web server tool (<https://mcule.com>) was utilized to carry out molecular docking, using the default binding site centers X: 7.2178, Y: 16.2957, and Z: 42.1167. The process of docking ligands with proteins and their interactions was investigated using the Discovery Studio visualizer V16.1.0.15350.⁴⁹

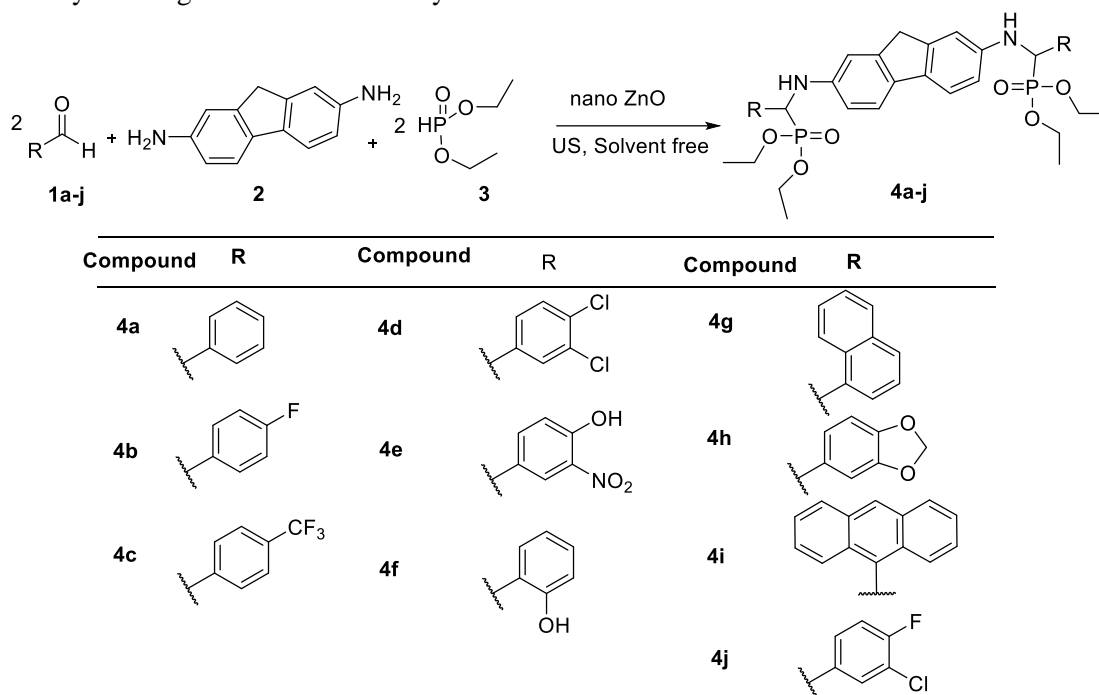
2.5. α -Amylase and α -Glucosidase Inhibitory Activity

Using a conventional methodology, all of the newly synthesized compounds were tested for their ability to inhibit α -amylase and α -glucosidase enzymes. (For a full procedure, refer to the Supplemental Materials). The half-maximal inhibitory concentration, or IC_{50} , is one of the most accurate indicators of a drug's effectiveness. In pharmacological research, it serves as a gauge of antagonist drug potency since it represents the quantity of medication needed to cut a biological process in half. Plotting the concentration (X-axis) against the percent inhibitory activity (Y-axis) allowed for the calculation of the IC_{50} values in this investigation. The x point on this graph becomes the IC_{50} value when the linear ($y=mx+c$) equation is applied to the $y=50$ value.

3. Results and Discussion

3.1. Chemistry

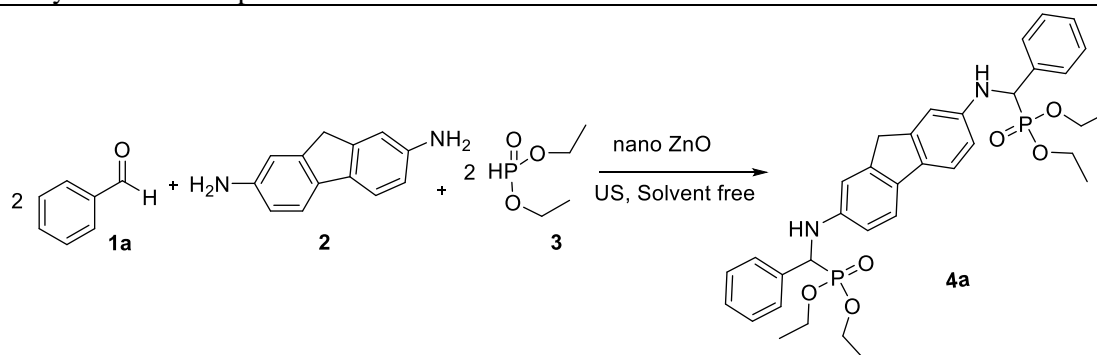
In this work, we synthesized a number of chemicals and assessed their ability to inhibit the enzymes α -amylase and α -glucosidase. Several aldehydes (**1a-j**), 9H-fluorene-2,7-diamine (**2**), and diethyl phosphite (**3**) were involved in a one-step K-F reaction that effectively produced the compounds (**4a-j**) found during the evaluation (93-97% yield). As shown in Scheme 1, the synthesis of α -AP (**4a-j**) was accomplished by ultrasonically utilizing nano ZnO as a catalyst.



Scheme 1. Ultrasound promoted nano ZnO catalyzed synthesis of α -Aps (**4a-j**)

For synthesis, benzaldehyde (**1a**), diethyl phosphite (**3**), and 9H-fluorene-2,7-diamine (**2**) were used in a model reaction. Tetraethyl(((9H-fluorene-2,7-diyl)bis(azanediyl))bis(phenylmethylene))bis(phosphonate) (**4a**) was the desired product of the initial reaction, which was carried out at 80°C in tetrahydrofuran (THF) without the use of a catalyst. The yield was poor (49%) over 30 hours (Table 1, entry 1). In order to improve the reaction efficiency, a variety of catalysts (2 mol%) were investigated, including *p*-toluenesulfonic acid (*p*-TSA), FeCl₃, TiO₂, ZnCl₂, LaCl₃, AlCl₃, CuCl₂, BF₃, BF₃.Et₂O, BF₃.SiO₂, and nano ZnO. Table 1 provides a summary of the findings (entries 2-12). The yield of **4a** increased from 67 to 79% after evaluating several catalysts, demonstrating the catalyst's critical role in the process. When THF was used as a solvent, nano ZnO produced a high product yield (79%) in just two hours, demonstrating its effectiveness among the catalysts studied (Table 1, entry 9).

Table 1. Synthesis of compound **4a** under various conditions.^a



Entry	Catalyst (mol%)	Solvent	Temp. (°C)	Time	Yield ^b (%)
1	Catalyst free	THF	80	30h	49
2	<i>p</i> -TSA (2)	THF	80	8h	67
3	FeCl ₃ (2)	THF	80	7h	68
4	TiO ₂ (2)	THF	80	8h	70
5	ZnCl ₂ (2)	THF	80	6h	72
6	LaCl ₃ (2)	THF	80	6h	71
7	AlCl ₃ (2)	THF	80	6h	73
8	CuCl ₂ (2)	THF	80	6h	69
9	BF ₃ (2)	THF	80	8h	70
10	BF ₃ .Et ₂ O (2)	THF	80	6h	72
11	BF ₃ .SiO ₂ (2)	THF	80	5 h	74
12	Nano ZnO (2)	THF	80	2h	79
13	Nano ZnO (2)	DCM	80	2.5h	75
14	Nano ZnO (2)	Toluene	110	3h	77
15	Nano ZnO (2)	Ethanol	40	2h	78
16	Nano ZnO (2)	Solvent-free	50	2h	84
17	Nano ZnO (2)	Solvent-free (Ultrasound)	Room temp.	7min	92
18	-	Solvent-free (Ultrasound)	Room temp.	12min	88

^aReaction of benzaldehyde, 9H-fluorene-2,7-diamine, and diethyl phosphite were selected as models to optimize reaction conditions

^bIsolated yield

A variety of solvents, including ethanol, toluene, and dichloromethane (DCM), were evaluated to determine how they affected the reaction. Nevertheless, there was no discernible rise in product yield (75-78%) (Table 1, entry 13-15). Furthermore, a favorable yield (84%) of the product was obtained in less than two hours when the reaction was carried out without the use of a solvent (Table 1, entry 16). Using nano ZnO (2 mol%), an ultrasound-assisted reaction was carried out without a solvent in order to further optimize the reaction conditions and reduce reaction time. As a result, **4a** produced a higher yield (92%) in 7 minutes (Table 1, entry 17).

It was investigated how the catalyst concentration (nano ZnO), which ranged from 2 to 10 mol%, affected the model reaction (Table 2, entries 1-5). Interestingly, using 6 mol% of the catalyst produced the highest yield of compound **4a**. Thus, during ultrasonication in a solvent-free environment, the effectiveness of a 6 mol% catalyst concentration was validated. The results are shown in Table 2.

Table 2. The effect of the catalyst quantity, nano ZnO to endorse the K-F reaction^a

Entry	Amount of Catalyst (mol%)	Time (min)	Yield ^b (%)
1	2	7	92
2	4	7	94
3	6	7	95
4	8	7	92
5	10	7	92

^aReaction of benzaldehyde, 9H-fluorene-2,7-diamine, and diethyl phosphite were chosen as replicas to optimize reaction environments

^bIsolated yield

Additionally, the recyclability of micro ZnO (6 mol%) was investigated. Dichloromethane (2 x 20 mL) was added to the reaction mixture and filtered after each cycle. The leftover catalyst was used for later runs after being dried and rinsed with chloroform. For the production of chemical **4a**, this procedure was repeated up to five times (Table 3, entries 1-5). As a result, during ultrasonication, micro ZnO (6 mol%) showed promise in catalyzing the reaction efficiently without the use of a solvent.

Table 3. Reusability of the catalyst, nano ZnO (6 mol%) for the synthesis of compound **4a**^a

Entry	Nano ZnO (6 mol%)	Time (min.)	Yield ^b (%)
1	First run	7	95
2	Second run	7	94
3	Third run	7	94
4	Forth run	7	92
5	Fifth run	7	91

^aReaction of benzaldehyde, 9H-fluorene-2,7-diamine, and diethylphosphite were selected as models to optimize reaction conditions

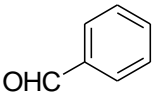
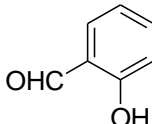
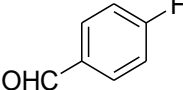
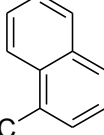
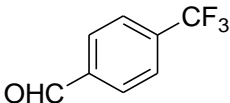
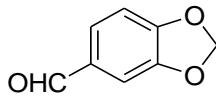
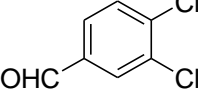
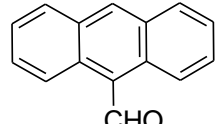
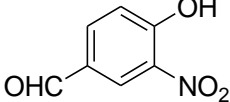
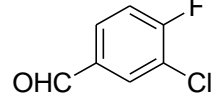
^bIsolated yield

After fine-tuning the reaction parameters, we proceeded to examine the versatility of this approach in synthesizing Alpha Aps (**4b-j**) (Scheme 1). This involved utilizing a range of aldehydes (**1b-j**), along with 9H-fluorene-2,7-diamine (**2**) and diethylphosphite (**3**), in the incidence of nano ZnO (6 mol%) without the use of solvent, employing ultrasonication. The outcomes of this investigation are summarized in Table 4.

As explained in the experimental section, elemental analysis and spectral data such as ³¹P, ¹H, and ¹³C NMR, IR, and LC-MS support the chemical structures of compounds **4a-j**. The experimental part contains the ³¹P NMR spectra, with Figure S 1 showing the spectrum of chemical **4a** as an example. The ³¹P NMR signals consistently showed up as singlets in the 24.2-15.2 ppm range for compounds **4a-j**.⁵⁰ The experimental part includes the proton NMR chemical shifts for compounds **4a-j**; Figure S 2 shows the spectrum of compound **4a**. Multiplet signals attributed to Ar-H were observed in the proton NMR spectra in the δ 8.39-6.67 ppm region. C-NH, P-CH, and CH₂ were represented by additional signals at 5.42, 3.95, and 3.73 ppm, respectively. P-O-CH₂CH₃'s methylene protons showed up as a multiplet, whereas compounds **4a-j**'s methyl protons resonated as triplets at δ 4.39 to 3.91 and δ 1.27 to 1.13 ppm, respectively.

All things considered; the spectrum results are in good agreement with the title compounds' suggested structures. The spectrum of compound **4a** is shown in Figure S 3 for reference, and experimental data for the ^{13}C NMR chemical shifts of compounds **4a-j** are presented. Distinct peaks corresponding to the P-CH carbon and methylene carbon of the fluorenyl group were observed at 56.71 and 37.3 ppm, respectively. In the ^{13}C NMR spectra of compounds **4a-j**, signals for P-O-CH₂-CH₃ and P-O-CH₂-CH₃ were noted at δ 64.07 to 62.85 and 14.85 to 13.88 ppm, respectively, confirming their presence. Additionally, the remaining carbon signals of the title compounds were detected within their anticipated regions. The infrared spectral analysis of the title compounds was showed to confirm the functional groups present. Compound **4a**'s IR spectrum, included in Figure S 4, serves as a representative example, while comprehensive data for compounds **4a-j** are provided in the experimental section. The IR spectral data endorse the functional groups existing in **4a-j**. The NH stretching vibrations of compounds **4a-j** were evidenced by distinctive infrared absorption bands in the range of 3354-3267 cm^{-1} . Characteristic absorption bands corresponding to the P=O functional group were observed in all compounds **4a-j**, within the region of 1223-1214 cm^{-1} . Additionally, stretching vibrations of P-O-C_{alip} were detected in compounds **4a-g**, appearing within the range of 1018-1009 cm^{-1} . These IR spectral findings confirm the presence of specific functional groups in compounds **4a-j**. Experimental data regarding the LC-MS analysis of compounds **4a-j** are detailed in the experimental section. The mass spectrum of compound **4a** is depicted in Figure S5 for reference. Notably, all title compounds exhibited M⁺ ions as base peaks, alongside isotopic cluster peaks displaying the anticipated ratios. The elemental analysis of Tetraethyl (((9H-fluorene-2,7-diyl)bis(azanediyl))bis(phenylmethylene))bis(phosphonate) (**4a**) is available in Figure S6 as representative paradigm. The Supplementary Materials contained typical spectra (^{31}P , ^1H , ^{13}C NMR, IR, mass and CHN analyses) of compound **4a** as representative of title compounds **4a-j** (Figure S 1-S 6).

Table 4. US mediated nano ZnO catalyzed synthesis of α -aminophosphonates (**4a-j**)^a

Compd.	Aldehyde	Time (min)	Yield ^b (%)	Compd.	Aldehyde	Time (min)	Yield ^b (%)
4a		5	95	4f		9	92
4b		5	93	4g		13	94
4c		7	96	4h		11	96
4d		9	94	4i		13	92
4e		9	95	4j		9	94

^aReaction of substituted aldehyde (1a-j), 9H-fluorene-2,7-diamine (2), and diethyl phosphite (3) in presence of nano ZnO (6 mol%) without solvent under Ultrasonication.

^bIsolated yield.

3.2. Pharmacology

3.2.1. *In Silico* ADME Analysis

Finding and creating new drugs is likely to favor compounds with low toxicity and high bioactivity. Molecular structure-based *in silico* ADMET (absorption, distribution, metabolism, excretion, and toxicity) property screening is one of the most effective ways to develop new drug candidates. Because ADME features may be predicted early in the drug development process, the rate of pharmacokinetic failure in clinical stages during the discovery phase is greatly reduced.⁵¹ SwissADME, which is available for use at <http://www.swissadme.ch>, was utilized to evaluate the ADME parameters of the suggested medications. The prediction was predicated on the structural and physicochemical benefits of the moieties. Table S 1 displays the physicochemical characteristics of molecules 4a-j (refer to the Supplemental materials).

When compared to acarbose, the metrics demonstrated a reasonable bioavailability score and were in good agreement with all relevant parameters for compounds 4a-j. Therefore, neither the tested compounds 4a-j nor the reference drug acarbose violate the Lipinski rule because their values are within the usual range. Table S 2 lists the ADME parameters for the recently manufactured medications. All of the substances were shown to have limited gastrointestinal absorption (GI).

Both human stomach absorption and passive blood-brain barrier (BBB) permeability (HIA) are demonstrated by the output of the BOILED-Egg model.⁵² The boiled egg schematic and the corresponding bio radar images of molecules 4a-j are shown in Figures S 7. (See in the Supplemental materials.) Since none of the compounds under investigation were absorbed, they were not BBB permeant, as evidenced by their identification outside the egg. Knowing whether substances are either substrates or non-substrates of the permeability glycoprotein (PGP) allows one to assess active efflux in biological membranes, particularly when it comes to occurrence from the gastrointestinal tract to the lumen.⁵³

The *p*-glycoprotein was expected to eradicate all designed molecules from the central nervous system. In a pharmacokinetic study, it is critical to forecast if an organic compound will cause significant drug interactions by inhibiting cytochromes (CYPs) such as CYP1A2, CYP2C19, CYP2C9, CYP2D6, and CYP3A4, as well as which isoenzymes would be affected.^{54,55} All the compounds except 4i, were predicted to be CYP3A4 inhibitors. Except for **4a** and **4b**, other compounds are not CYP2D6 inhibitors. Except **4e**, all other molecules were predicted to be non-inhibitors of CYP2C9. Except **4d**, **4e**, **4i** and **4j**, all other molecules were also found to be CYP2C19 inhibitors. The reference drug, acarbose, is found to be non-inhibitor of all of these isoenzymes.

Multiple linear regression is a methodology for predicting the skin permeability coefficient (K_p). It is based on Potts and Guy's⁵⁶ discovery of a linear association between K_p and molecule size and lipophilicity ($R^2=0.67$). The compounds 4e, 4f, and 4h were found to have the largest negative log K_p values and the lowest skin permeability among the title compounds. The reference drug exhibited the lowest skin permeability and the greatest log K_p of all the compounds tested (-16.29). The results are shown in Table S 2. (See the Supplemental Materials for Table S 2).

Predicting drug-likeness variables can help with the qualitative identification of a compound that turns out to be a high-bioavailability oral medicine. We employed five rules to assess the oral bioavailability and drug-likeness of the synthesized compounds: Lipinski⁵⁷, Ghose⁵⁸, Veber⁵⁹, Egan⁶⁰, and Muegge⁶¹. All of the molecules, with a few exceptions, followed the five principles. Table 5 lists the features of compounds 4a-j that are relevant to drug similarity. The compounds **4a** and **4f** had a bioavailability value of 0.55, while the remaining molecules had a bioavailability score of 0.17, including acarbose. The lack of warnings for pan assay interference substances (PAINS) suggests that the lead molecules' pharmacokinetic profile is favorable, with the exception of 4f. When compared to the reference drug, the majority of the compounds displayed favorable physicochemical, pharmacokinetic, and drug-like properties.

Table 5. Drug likeness properties of compounds **4a-j**

Compd.	Lipinski violations	Ghose violations	Veber violations	Egan violations	Muegge violations	B.S	PAINS alerts	S.A.
4a	1	4	1	1	3	0.55	0	5.91
4b	2	4	1	1	3	0.17	0	5.9
4c	2	4	1	1	4	0.17	0	6.14
4d	2	4	1	1	3	0.17	0	5.96
4e	2	4	2	2	5	0.17	0	6.2
4f	1	4	2	2	4	0.55	1	5.96
4g	2	4	1	1	3	0.17	0	6.42
4h	2	4	2	2	4	0.17	0	6.2
4i	2	4	1	1	4	0.17	0	6.93
4j	2	4	1	1	3	0.17	0	5.95
Acarbose	3	4	1	1	5	0.17	0	7.34

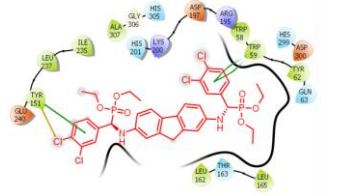
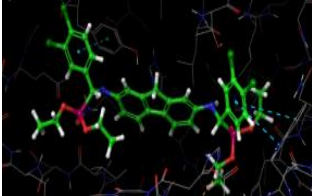
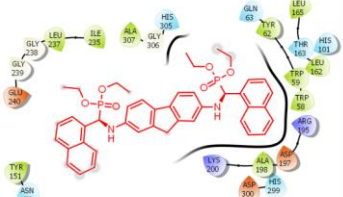
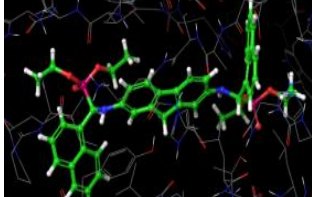
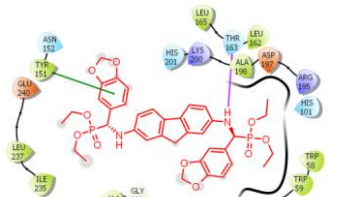
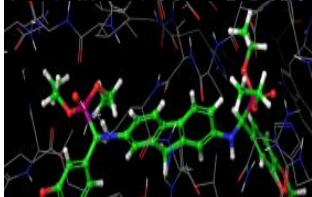
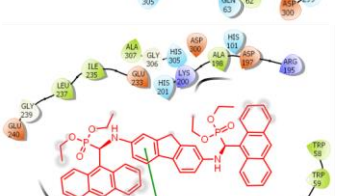
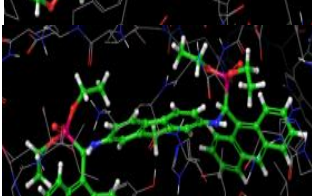
B.S.: Bioavailability Score; S.A.: Synthetic Accessibility

3.2.1. In-silico Molecular Docking Study on α -Amylase Enzyme

The designed molecules underwent in silico screening to evaluate their binding affinity with the pancreatic α -amylase enzyme, utilizing the 1-click docking online server tool (<http://mcule.com/apps/1-click-docking/>) authorized by the AutoDock Vina docking algorithm.⁶² The screening outcomes revealed that all molecules exhibited superior or comparable binding energies (-8.9 to -7.5 kcal/mol) compared to the reference drug, acarbose (-8.2 kcal/mol). Detailed data on binding energies and the corresponding bonding poses of complexes are presented in Table S 3. (See supplemental materials).

All screened molecules **4a-j** exhibited favorable docking with binding energies ranging from -7.5 to -8.9 kcal/mol. Notably, compounds **4d**, **4g**, **4h**, and **4i** displayed higher binding energies than the reference drug, as indicated in **Table S 1**. (See supplemental materials) The docking scores followed the order: **4i** > **4d** = **4g** > **4h** > **4a** > **4f** > **4e** > **4j** > **4b** > **4c**. For instance, in molecule **4d**, the phenyl group engaged in π - π stacking with Tyr151 and Trp59, while a halogen bond formed between the chlorine atom and Tyr151. Hydrophobic contacts were also observed with residues Leu162, Leu165, Tyr62, Trp59, Trp58, Ala307, Ile237, and Tyr151. Similarly, molecule **4g** exhibited hydrophobic interactions with residues such as Leu165, Leu162, Tyr62, Trp58, Trp59, Ala198, Tyr151, Ile237, Ile235, and Ala307. In molecule **4h**, a hydrogen bond was identified between the hydrogen atom of the amine and Thr163, with π - π stacking observed between the 2H-1,3-benzodioxol-5-yl group and Tyr151. Hydrophobic contacts were also formed with Leu237, Ile235, Tyr151, Ala307, Trp58, Trp59, Tyr62, Ala198, Leu162, and Leu165. In molecule **4i**, the fluorenyl group engaged in π - π stacking with Tyr151, along with hydrophobic contacts with residues Leu237, Ile235, Ala307, Ala198, Trp58, Trp59, Tyr62, Tyr151, Leu162, and Leu165. Detailed 2D & 3D ligand diagrams depicting the binding contacts of molecules **4d**, **4g**, **4h**, and **4i** with the target enzyme are provided in Table 6.

Table 6. 2D Lig Plot and 3D images of compounds **4d**, **4g**, **4h**, and **4i**

Compound	2D structure	3D structure
4d		
4g		
4h		
4i		

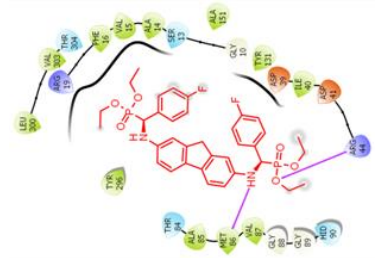
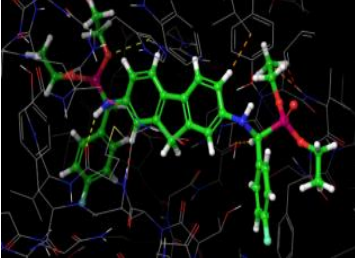
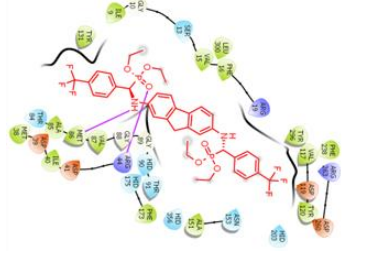
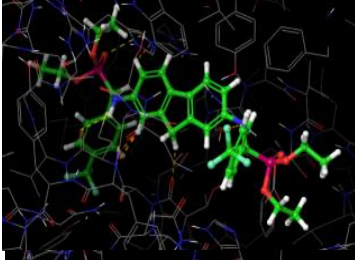
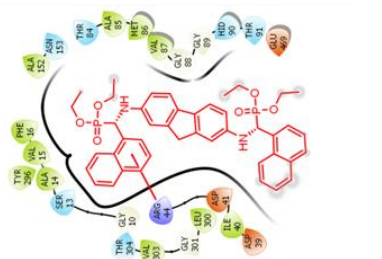
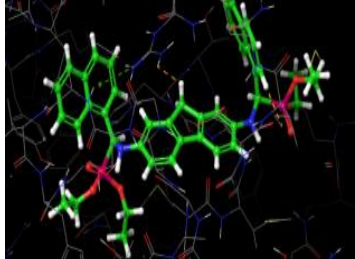
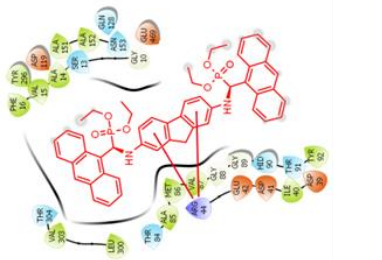
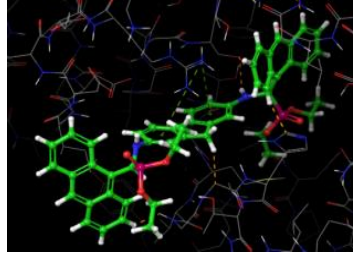
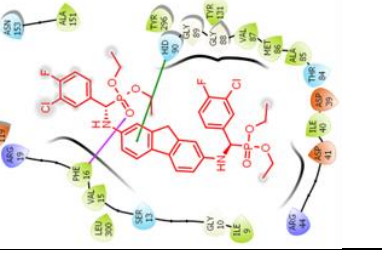
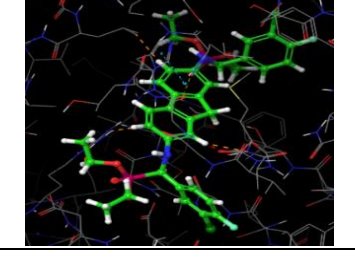
3.2.2. In-silico Molecular Docking Study on α -Glucosidase Enzyme

All the synthesized molecules underwent in silico screening to evaluate their binding affinity with pancreatic α -glucosidase enzyme using the 1-click docking online server tool, authorized by the AutoDock Vina docking algorithm.⁶² The results revealed that all molecules exhibited better or nearly equal binding energies (-9.2 to -7.2 kcal/mol) compared to the reference drug, acarbose (-7.8 kcal/mol). Detailed data on binding energies and corresponding bonding poses of complexes are provided in Table S 3. (See supplemental materials)

Among the screened molecules (**4a-j**), favorable docking was observed with binding energies ranging from -7.2 to -9.2 kcal/mol. Notably, molecules **4b**, **4c**, **4g**, **4i**, and **4j** displayed equal or higher binding energies compared to the reference drug. The docking order of the title compounds was as follows: **4i** > **4g** > **4c** > **4j** > **4b** > **4f** > **4e** = **4h** > **4d** > **4a**. For instance, in molecule **4b**, hydrogen bonds were formed between the amine group hydrogen atom and Met86, and between the oxygen atom of the P-O-Et group and Arg44. Additionally, hydrophobic contacts were observed with residues Val87, Met86, Ala85, Tyr296, Leu300, Val303, Phe16, Val15, Ala14, Ala151, Tyr131, and Ile40. In molecule **4c**, similar hydrogen bonds were formed along with hydrophobic contacts with residues Tyr131, Ile9, Val15, Leu300, Phe16, Tyr296, Val117, Tyr120, Phe238, Ala151, Fhe173, Val87, Met86, Ala85, Ile40, and Met38. Molecule **4g** displayed hydrophobic contacts with residues Ile40, Leu300, Val303, Ala14, Val15, Phe16, Tyr296, Ala152, Ala85, Met86, and Val87, while in molecule **4i**, the fluorenyl group engaged in a π -cation interaction with Arg44, along with hydrophobic contacts with residues Ile40, Tyr92, Val87, Met86, Ala85, Leu300, Val303, Phe16,

Val15, Ala14, Tyr296, and Ala151. Similarly, molecule **4j** formed a hydrogen bond between the oxygen atom of the P-O-Et group and Phe16, along with hydrophobic contacts with Ile9, Leu300, Val15, Phe16, Ala151, Tyr296, Tyr131, Val87, Met86, Ala85, and Ile40. Detailed 2D & 3D ligand diagrams illustrating the binding contacts of molecules **4b**, **4c**, **4g**, **4i**, and **4j** with the target enzyme are provided in Table 7.

Table 7. 2D Lig Plot and 3D images of compounds **4b**, **4c**, **4g**, **4i**, and **4j**

Compound	2D structure	3D structure
4b		
4c		
4g		
4i		
4j		

3.2.3. *In-vitro* α -Amylase and α -Glucosidase Inhibitory Assay

Employing a modified version of a well-established procedure,^{63,64} the synthesized compounds underwent *in vitro* testing to assess their potential as α -amylase inhibitors. The screening was conducted at various doses ranging from 25 to 250 $\mu\text{g/mL}$. The majority of the compounds demonstrated effective inhibition of the target enzyme. Notably, compounds **4d** (IC_{50} , 102.2 \pm 0.3 $\mu\text{g/mL}$), featuring a 3,4-dichlorophenyl group, **4h** (IC_{50} , 102.9 \pm 0.4 $\mu\text{g/mL}$), with a 2H-1,3-benzodioxol-5-yl moiety, and **4i** (IC_{50} , 103.9 \pm 0.5 $\mu\text{g/mL}$), bearing an anthracen-9-yl substituent, exhibited the strongest inhibitory activity compared to the reference medication, acarbose (IC_{50} , 106.5 \pm 0.6 $\mu\text{g/mL}$). Compound **4a**, with a phenyl substituent (IC_{50} , 111.8 \pm 0.7 $\mu\text{g/mL}$), **4f**, with a 2-hydroxyphenyl substituent (IC_{50} , 114.9 \pm 0.8 $\mu\text{g/mL}$), and **4g**, with a naphthalen-1-yl substituent (IC_{50} , 109.6 \pm 0.3 $\mu\text{g/mL}$) displayed notable inhibitory action compared to the standard. The remaining compounds exhibited moderate to good enzyme inhibition, with IC_{50} values ranging from 120.4 \pm 0.3 to 166.2 \pm 0.6 $\mu\text{g/mL}$. Figures S 8 illustrate the percent inhibition values for all compounds **4a-j**. (See supplemental materials)

Utilizing an adapted methodology⁶⁵ the synthesized compounds underwent *in vitro* testing to assess their potential as α -glucosidase inhibitors. The screening was conducted across doses ranging from 25 to 250 $\mu\text{g/mL}$. The majority of the compounds exhibited significant inhibition against the target enzyme. Notably, compound **4g**, featuring a naphthalen-1-yl substituent (IC_{50} , 87.5 \pm 0.3 $\mu\text{g/mL}$), **4h** (IC_{50} , 91.7 \pm 0.8 $\mu\text{g/mL}$), bearing a 2H-1,3-benzodioxol-5-yl moiety, and **4i** (IC_{50} , 90.1 \pm 0.5 $\mu\text{g/mL}$), with an anthracen-9-yl moiety, demonstrated the highest inhibitory activity compared to the reference drug, acarbose (IC_{50} , 92.8 \pm 0.9 $\mu\text{g/mL}$). Compounds **4c**, featuring a trifluoromethyl substituent (IC_{50} , 95.4 \pm 0.2 $\mu\text{g/mL}$), **4a** (IC_{50} , 106.7 \pm 0.1 $\mu\text{g/mL}$), bearing a phenyl substituent, and **4d** (IC_{50} , 106.7 \pm 0.1 $\mu\text{g/mL}$), featuring a 3,4-dichlorophenyl substituent, exhibited notable inhibitory activity. The remaining compounds displayed moderate to good enzyme inhibition, with IC_{50} values ranging from 117.0 \pm 0.4 to 141.9 \pm 0.1 $\mu\text{g/mL}$. Figures S 9 presents the results regarding percent inhibition values of all compounds **4a-j**. (See supplemental materials)

Table 8 represents the results regarding IC_{50} values of all compounds **4a-j**, for α -amylase and α -glucosidase inhibitory assays respectively.

Table 8. IC_{50} values of compounds **4a-j**

Compound	α -amylase	α -glucosidase
	inhibition activity	inhibition activity
	IC_{50}	IC_{50}
4a	111.8	106.7
4b	150.7	117.0
4c	166.2	95.4
4d	102.2	101.7
4e	120.4	127.0
4f	114.9	141.9
4g	109.6	87.5
4h	102.9	91.7
4i	103.9	90.1
4j	153.6	136.3
Acarbose	106.5	92.8

The structure-activity relationship (SAR) analysis of synthesized compounds for α -amylase and α -glucosidase inhibition emphasizes the importance of substituent type and position in influencing inhibitory potency. Compounds with hydrophobic and π -conjugated groups, such as **4d** (3,4-dichlorophenyl, IC_{50} : 102.2 $\mu\text{g/mL}$), **4h** (2H-1,3-benzodioxol-5-yl, IC_{50} : 102.9 $\mu\text{g/mL}$), and **4i** (anthracen-9-yl, IC_{50} : 103.9 $\mu\text{g/mL}$), superior to the reference drug, acarbose (IC_{50} : 106.5 $\mu\text{g/mL}$). These findings indicate that hydrophobic interactions and π - π stacking considerably increase binding affinity to the enzyme's active region. Similarly,

molecules such as **4a** (phenyl), **4f** (2-hydroxyphenyl), and **4g** (naphthalen-1-yl) showed high activity due to their capacity to generate moderate hydrophobic or hydrogen-bonding contacts.

The most potent inhibitors for α -glucosidase were **4g** (naphthalen-1-yl, IC_{50} : 87.5 μ g/mL), **4h** (2H-1,3-benzodioxol-5-yl, IC_{50} : 91.7 μ g/mL), and **4i** (anthracen-9-yl, IC_{50} : 90.1 μ g/mL), with activity surpassing acarbose (IC_{50} : 92.8 μ g/mL). The compounds showed strong π - π interactions and hydrophobic binding. Electronegative substituents, such as the trifluoromethyl group in **4c**, significantly increased α -glucosidase inhibitory activity (IC_{50} : 95.4 μ g/mL) via stabilizing electrostatic interactions. These compounds' increased inhibitory activity is attributed to their bulky hydrophobic substituents, π -rich systems, and polar groups that promote hydrogen bonding. The findings highlight the significance of these interactions in optimizing enzyme inhibition, with compounds **4d**, **4h**, and **4i** emerging as interesting candidates for further development as dual inhibitors for diabetes management.

4. Conclusion

A more environmentally friendly synthesis method was developed for producing novel Bis(alpha Aps) **4a-j**. This was achieved through a one-pot Kabachnik-Fields reaction, yielding high product yields under ultrasound-mediated, solvent-free conditions with nano ZnO as a reusable catalyst. Before synthesis, the compounds were strategically designed for molecular docking simulations to identify the most promising candidates for drug development. Molecular docking analysis revealed that all examined compounds effectively inhibited the target enzyme. The synthesis of compounds showing strong inhibition of α -amylase and α -glucosidase enzymes was prioritized, resulting in reduced drug development costs, time, and chemical waste. The newly synthesized compounds were tested in vitro for their α -amylase and α -glucosidase inhibitory activities using standard spectrophotometric methods. Compared to the reference drug, compounds **4h** and **4i** showed superior inhibition, while compounds **4a** and **4e** exhibited comparable inhibition against the α -amylase enzyme. Against the α -glucosidase enzyme, compounds **4a**, **4h**, and **4i** demonstrated superior inhibition, while **4g** showed comparable inhibition to the reference drug. These results suggest that the synthesized compounds hold promise as next-generation α -amylase and α -glucosidase inhibitors for diabetes treatment.

Acknowledgements

Authors acknowledge Dr. C. Naga Raju, Department of Chemistry, S. V. University, Tirupati for his constant support in completing this work.

Supporting Information

Supporting information accompanies this paper on <http://www.acgpubs.org/journal/organic-communications>

ORCID

Meson Haji Basha: [0000-0001-8287-2416](https://orcid.org/0000-0001-8287-2416)

Chennamsetty Subramanyam: [0000-0002-0422-6096](https://orcid.org/0000-0002-0422-6096)

C. Gladis Raja Malar: [0000-0001-8608-9023](https://orcid.org/0000-0001-8608-9023)

Katara Kiran Kumar: [0000-0001-8612-5776](https://orcid.org/0000-0001-8612-5776)

Mohan Seelam: [0000-0002-5819-3576](https://orcid.org/0000-0002-5819-3576)

Vedula Naga Lakshmi: [0000-0001-5474-5815](https://orcid.org/0000-0001-5474-5815)

Kammela Prasada Rao: [0000-0003-1987-9222](https://orcid.org/0000-0003-1987-9222)

References

- [1] International Diabetes Federation. (2021). IDF Diabetes Atlas (10th ed.). Retrieved from <https://www.idf.org>.
- [2] Ceriello, A. Postprandial hyperglycemia and diabetes complications: Is it time to treat? *Diabetes*, **2010**, 58(1), 1-7.

- [3] Van de Laar, F. A. Alpha-glucosidase inhibitors in the early treatment of type 2 diabetes. *Vascular Health and Risk Management*, **2008**, *4*(6), 1189-1195.
- [4] Vora, J.; Patel, S.; Sinha, S. Advances in molecular docking as a tool for drug discovery and development. *Front. Pharmacol.* **2019**, *10*, 127.
- [5] Wang, Y.; Cobo, A.A.; Franz, A.K. Recent advances in organocatalytic asymmetric multicomponent cascade reactions for enantioselective synthesis of spirooxindoles. *Org. Chem. Front.* **2021**, *8*, 4315-4348.
- [6] Lemos, B.C.; Venturini Filho, E.; Fiorot, R.G.; Medici, F.; Greco, S.J.; Benaglia, M. Enantioselective Povarov reactions: an update of a powerful catalytic synthetic methodology. *Eur. J. Org. Chem.* **2022**, *2022*(2), e202101171.
- [7] Fouad, M.A.; Abdel-Hamid, H.; Ayoup, M.S. Two decades of recent advances of Ugi reactions: synthetic and pharmaceutical applications. *RSC Adv.* **2020**, *10*, 42644-42681.
- [8] Knapp, J.M.; Kurth, M.J.; Shaw, J.T.; Younai, A. Strategic applications of multicomponent reactions in diversity-oriented synthesis; Trabocchi, A., Ed.; Wiley: New York, NY, USA, 2013; pp. 29-57.
- [9] Schreiber, S.L. Target-oriented and diversity-oriented organic synthesis in drug discovery. *Science* **2000**, *287*, 1964-1969.
- [10] Kraicheva, I.; Vodenicharova, E.; Shivachev, B.; Nikolova, R.; Kril, A.; Topashka-Ancheva, M.; Iliev, I.; Georgieva, A.; Gerasimova, T. S.; Tosheva, T.; Tashev, E.; Tsacheva, I.; Troev, K. *Phosphor. Sulfur Silic. Relat. Elem.* **2013**, *188*(11), 1535-1547.
- [11] Sadik, S. M.; Santhisudha, S.; Mohan, G.; Reddy, N. M.; Lakshmi, P. S.; Rajasekhar, A.; Reddy, C. S. Palladium acetate-catalysed one-pot green synthesis of bis α -aminophosphonates. *Res. Chem. Intermed.* **2019**, *45*(3), 1401-1420.
- [12] Mulla, A. R. S.; Pathan, M. Y.; Chavan, S. S.; Gample, S. P.; Sarkar, D. Highly efficient one-pot multi-component synthesis of α -aminophosphonates and bis- α -aminophosphonates catalyzed by heterogeneous reusable silica supported dodecatungstophosphoric acid (DTP/SiO₂) at ambient temperature and their antitubercular evaluation against *Mycobacterium tuberculosis*†. *RSC. Adv.* **2014**, *4*, 7666-7672.
- [13] Pavan Phani Kumar, M.; Anuradha, V.; Gladis Raja Malar, C.; Subramanyam, Ch.; Subrahmanyam, T.; Nagalakshmi, V. In silico molecular docking study and nano TiO₂-SiO₂ catalyzed microwave facilitated synthesis of new bis(α -aminophosphonates) as potential anti-diabetic agents. *Phosphor. Sulfur Silic. Relat. Elem.* **2023**, *198*(10), 808-821.
- [14] Rezaei, Z.; Firouzabadi, H.; Iranpoor, N.; Ghaderi, A.; Jafari, M. R. A.; Jafari, A.; Zare, H. R. Design and one-pot synthesis of α -aminophosphonates and bis(α -aminophosphonates) by iron(III) chloride and cytotoxic activity. *Eur. J. Med. Chem.* **2009**, *44*, 4266-4275.
- [15] Milen, M.; Balogh, P. A.; Kangyal, R.; Dancso, A.; Frigyes, D.; Keglevich, G. T3P®-mediated one-pot synthesis of bis(α -aminophosphonates). *Heteroat. Chem.* **2014**, *25*(4), 245-255.
- [16] Kaur, T.; Saha, D.; Singh, N.; Singh, U. P.; Sharma, A. A rapid one-pot five component sequential access to novel imidazo[2,1-b]thiazinyl- α -aminophosphonates. *Chem. Select.* **2016**, *1*(3), 434-439;
- [17] Abdel-Rahman, R. M.; Ali, T. E. Synthesis and biological evaluation of some new polyfluorinated 4-thiazolidinone and α -aminophosphonic acid derivatives. *Monatsh. Chem.* **2013**, *144*(8), 1243-1252.
- [18] Li, X. C.; Gong, S. S.; Zeng, D. Y.; You, Y. H.; Sun, Q. Highly efficient synthesis of α -aminophosphonates catalyzed by hafnium(IV) chloride. *Tetrahedron Lett.* **2016**, *57*(16), 1782-1785;
- [19] Han, W.; Mayer, P.; Ofiala, R. A. Iron-catalyzed oxidative mono- and bis-phosphonation of n,n-dialkylanilines. *Adv. Synth. Catal.* **2010**, *352*(10), 1667-1676.
- [20] Prishchenko, A. A.; Livantsov, M. V.; Novikova, O. P.; Livantsova, L. I.; Petrosyan, V. S. Synthesis of bis- and tris-organophosphorus substituted amines and amino acids with PCH₂N Fragments. *Heteroat. Chem.* **2010**, *21*, 430-440.
- [21] Lewkowski, J.; Karpowicz, R.; Mazur, A. Addition of Phosphites to N,N-Diferrocenylidene-1,3-phenylenedimethylamine and N,N-Diferrocenylidene-1,3-cyclohexylenedimethylamine: Synthesis of corresponding model bis-aminophosphonates. *Phosphor. Sulfur Silic. Relat. Elem.* **2010**, *185*, 2108-2112.
- [22] Lewkowski, J.; Tokarz, P.; Lis, T.; Slepokura, K. Stereoselective addition of dialkyl phosphites to disalicylaldimines bearing the (R,R)-1,2-diaminocyclohexane moiety. *Tetrahedron* **2014**, *70*, 810-816.
- [23] Malamiri, F.; Khaksar, S. Pentafluorophenylammonium triflate (PFPAT): A new organocatalyst for the one-pot three-component synthesis of α -aminophosphonates. *J. Chem. Sci.* **2014**, *126*, 807-811.
- [24] Yu, Y.Q.; Xu, D.Z. A Simple and green procedure for the one-pot synthesis of α -aminophosphonates with quaternary ammonium salts as efficient and recyclable reaction media. *Synthesis* **2015**, *47*, 1869-1876.
- [25] Xu, W.; Zhang, S.; Yang, S.; Jin, L. H.; Bhadury, P. S.; Hu, D.Y.; Zhang, Y. Asymmetric synthesis of α -aminophosphonates using the inexpensive chiral catalyst 1,1'-binaphthol phosphate. *Molecules* **2010**, *15*, 5782-5796.

- [26] Bhaskar Reddy, M.; Gal Reddy, P.; Manjula A. Synthesis of Tröger's base bis(α -aminophosphonate) derivatives. *Arkivoc* **2016**, (iv), 246-260.
- [27] Ordonez, M.; Cabrera, H. R.; Cativiela, C. An overview of stereoselective synthesis of α -aminophosphonic acids and derivatives. *Tetrahedron* **2009**, *65*, 17-49.
- [28] Rim, A.; Samia, G.L.; Emilie, K.; Martial, T.; Louisa, A.Z. Diastereoselective synthesis of bis(α -aminophosphonates) by lipase catalytic promiscuity. *New J. Chem.* **2019**, *43*, 8153-8159.
- [29] Hossein, E.; Mahdi, M.; Maede, H.; Majid, M.E. *Phosphor. Sulfur Silic. Relat. Elem.* **2015**, *190*(10), 1606-1620.
- [30] Bakthavatchala Reddy, N.; Syama Sundar, C.; Satheesh Krishna, B.; Santhisudha, S.; Sreelakshmi, P.; Sandip Kumar, N.; Suresh Reddy, C. Cellulose-SO₃H catalyzed synthesis of bis(α -aminophosphonates) and their antioxidant activity. *Org. Commun.* **2017**, *10*(1), 46-55.
- [31] Tarik El-Sayed Ali, Synthesis and characterization of novel bis-(α -aminophosphonates) with terminal chromone moieties. *Arkivoc* **2008**, (ii), 71-79.
- [32] Souii, I.; Sanhoury, M.A.; Vicario, J.; Jiménez-Aberásturi, X.; Efrít, M.L.; M'rabet, H.; de los Santos, J.M. Synthesis and characterization of a new series of bis(allylic- α -aminophosphonates) under mild reaction conditions. *Molecules* **2023**, *28*, 4678.
- [33] Tajti, A.; Balint, E.; Keglevich, G. Microwave-assisted synthesis of α -aminophosphonates and related derivatives by the Kabachnik-Fields reaction. *Phosphor. Sulfur Silic. Relat. Elem.* **2019**, *194*, 379-381.
- [34] Bálint, E.; Tajti, Á.; Tripolszky, A.; Keglevich, G. Synthesis of α -aminophosphonates and related derivatives under microwave conditions. *Proceedings* **2017**, *1*, 1-6.
- [35] Xia, M.; Lu, Y. Ultrasound-assisted one-pot approach to α -amino phosphonates under solvent-free and catalyst-free conditions. *Ultrason. Sonochem.* **2007**, *14*, 235-240;
- [36] Kirti, S. N.; Bapurao, B.; Shingate Murlidhar, S. S. Solvent-free sonochemical preparation of α -aminophosphonates catalyzed by 1-hexanesulphonic acid sodium salt. *Ultrason. Sonochem.* **2010**, *17*(5), 760-763.
- [37] Hosseini Sarvari, M.; Etemad, S. Nanosized zinc oxide as a catalyst for the rapid and green synthesis of β -phosphono malonates. *Tetrahedron* **2008**, *64*, 5519-5523.
- [38] Hosseini-Sarvari, M.; Sharghi, H.; Etemad, S. Nanocrystalline ZnO for Knoevenagel Condensation and Reduction of the Carbon,Carbon Double Bond in Conjugated Alkenes. *Helv. Chim. Acta.* **2008**, *91*(4), 715-724.
- [39] Mirjafary, Z.; Saeidian, H.; Sadeghi, A.; Moghaddam, F.M. ZnO nanoparticles: An efficient nanocatalyst for the synthesis of β -acetamido ketones/esters via a multi-component reaction. *Catal. Commun.* **2008**, *9*, 299-306.
- [40] Kassae, M.Z.; Masrouri, H.; Movahedi, F. ZnO-nanoparticle-promoted synthesis of polyhydroquinoline derivatives via multicomponent Hantzsch reaction. *Monatsh. Chem.* **2010**, *141*, 317-322.
- [41] Singh, N.; Mehra, R.M.; Kapoor, A. Synthesis and characterization of ZnO nanoparticles. *J. Nano-Eletron. Phys.* **2011**, *3*, 132-139.
- [42] Seema, R.; Poonam, S.; Shishodia, P.K.; Mehra, R.M. Synthesis of nanocrystalline ZnO powder via sol-gel route for dye-sensitized solar cells. *Sol. Energ. Mat. Sol. Cells* **2008**, *92*(12), 1639-1645.
- [43] Thaslim Basha, SK.; Rasheed, S.; Sekhar, K.C.; Raju, C.N.; Ali, M.S.; Rao, C.A. Ultrasonicated, nano-ZnO catalyzed green synthesis of α -hydroxyphosphonates and their antioxidant activity. *Phosphor. Sulfur Silic. Relat. Elem.* **2014**, *189*, 1546-1556.
- [44] Subramanyam, Ch.; Thaslim Basha, Sk.; Madhava, G.; Nayab Rasool, Sk.; Adam, Sk.; Durga Srinivasa Murthy, S; Naga Raju, C. Synthesis, spectral characterization and bioactivity evaluation of novel α -aminophosphonates. *Phosphor. Sulfur Silic. Relat. Elem.* **2017**, *192* (3), 267-270.
- [45] Sujatha, B.; Mohan, S.; Subramanyam, Ch.; Prasada Rao, K. Microwave-assisted synthesis and anti-inflammatory activity evaluation of some novel α -aminophosphonates. *Phosphor. Sulfur Silic. Relat. Elem.* **2017**, *192*(10), 1110-1113.
- [46] Altaff, SK. Md.; Raja Rajeswari, T.; Subramanyam, Ch. Synthesis, α -amylase inhibitory activity evaluation and *In silico* molecular docking study of some new phosphoramidates containing heterocyclic ring. *Phosphor. Sulfur Silic. Relat. Elem.* **2021**, *196*(4), 389-397.
- [47] Haji Basha, M.; Subramanyam, Ch.; Gladis Raja Malar, C.; Someswara Rao, S.; Prasada Rao, K. Nano TiO₂.SiO₂ catalyzed, microwave assisted synthesis of new α -aminophosphonates as potential anti-diabetic agents: In silico ADMET and molecular docking study. *Org. Commun.* **2022**, *15*(2), 167-183.
- [48] Priyadarsini, P.; Madhava Rao, V.; Hanumatha Rao A.; Subramanyam Ch.; Ranganayakulu Y. A simple, efficient synthesis and molecular docking studies of 2-styrylchromones, *Org. Commun.* **2021**, *14*(2), 121-132.
- [49] Madhu Kumar Reddy, K.; Peddanna, K.; Varalakshmi, M.; Bakthavatchala Reddy, N.; Sravya, G.; Grigory, V. Z.; Reddy, S.C. Ceric ammonium nitrate (CAN) catalyzed synthesis and α -glucosidase activity of some novel tetrahydropyridine phosphonate derivatives *Phosphor. Sulfur Silic. Relat. Elem.* **2019**, *194*, 812-819.
- [50] Quin, L. D.; Verkade, J. G. Phosphorus-31 NMR Spectral Properties Compound Characterization and Structural Analysis; VCH Publishers: New York, **1994**.

- [51] Hay, M.; Thomas, D. W.; Craighead, J. L.; Economides, C.; Rosenthal, J. Clinical development success rates for investigational drugs. *Nature Biotechnol.* **2014**, *32*, 40-51.
- [52] Daina, A.; Zoete, V. A boiled-egg to predict gastrointestinal absorption and brain penetration of small molecules. *Chem. Med. Chem.* **2016**, *11*, 1117-1121.
- [53] Montanari, F.; Ecker, G. F. Prediction of drug-ABC-transporter interaction-recent advances and future challenges. *Adv. Drug Deliv. Rev.* **2015**, *86*, 17-26.
- [54] Hollenberg, P. F. Characteristics and common properties of inhibitors, inducers, and activators of CYP enzymes. *Drug Metab. Rev.* **2002**, *34*, 17-35.
- [55] Shiew-Mei, H.; John, M. S.; Lei, Z.; Kellie, S. R.; Srikanth, N.; Robert, T. Abraham, S.; Al Habet, S.; Bajewa, R.K.; Burckart, G.J. *et al.* New era in drug interaction evaluation: US food and drug administration update on CYP enzymes, transporters, and the guidance process. *J. Clin. Pharmacol.* **2008**, *48*, 662-670.
- [56] Potts, R. O.; Guy, R. H. Predicting Skin Permeability. *Pharm. Res.* **1992**, *9*, 663-669.
- [57] Lipinski, C.A.; Lombardo, F.; Dominy, B.W.; Feeney, P.J. Experimental and computational approaches to estimate solubility and permeability in drug discovery and development settings. *Adv. Drug Del. Rev.* **2001**, *46*, 3-26.
- [58] Ghose, A.K.; Viswanadhan, V.N.; Wendoloski, J.J. Prediction of hydrophobic (lipophilic) properties of small organic molecules using fragmental methods: An analysis of ALOGP and CLOGP methods. *J. Phys. Chem. A.* **1998**, *102*, 3762-3772.
- [59] Veber, D.F.; Johnson, S.R.; Cheng, H.Y.; Smith, B.R.; Ward, K.W.; Kopple, K.D. Molecular properties that influence the oral bioavailability of drug candidates. *J. Med. Chem.* **2002**, *45*, 2615-2623.
- [60] Egan, W.J.; Lauri, G. Prediction of intestinal permeability. *Adv. Drug Del. Rev.* **2002**, *54*, 273-289.
- [61] Muegge, I.; Heald, S.L.; Brittelli, D. Simple selection criteria for drug-like chemical matter. *J. Med. Chem.* **2001**, *44*, 1841-1846.
- [62] Trott, O.; Olson, A.J. Auto Dock Vina: improving the speed and accuracy of docking with a new scoring function, efficient optimization and multithreading. *J. Comput. Chem.* **2010**, *31*, 455-461.
- [63] Nickavar, B.; Amin, G. Enzyme assay guided isolation of an alpha-amylase inhibitor flavonoid from vaccinium arctostaphylos leaves. *Iran J. Pharm. Res.* **2011**, *10*, 849-853.
- [64] Patil, V. S.; Nandre, K. P.; Ghosh, S.; Rao, V. J.; Chopade, B. A.; Sridhar, B.; Bhosale, S. V.; Bhosale, S. V. Synthesis, crystal structure and anti-diabetic activity of substituted (E)-3-(benzo[d]thiazol-2-ylamino)phenylprop-2-en-1-one. *Eur. J. Med. Chem.* **2013**, *59*, 304-309.
- [65] Kim, J.S.; Hyun, T.K.; Kim, M.J. The inhibitory effects of ethanol extracts from sorghum, foxtail millet and proso millet on α -glucosidase and α -amylase activities. *Food Chem.* **2011**, *124*, 1647-1651.

ACG
publications

© 2024 ACG Publications